

PAPER DETAILS

TITLE: Preparation of Cerium Oxide Nanoparticles: An Efficient Catalyst to the Synthesis of Dimeric Disulphide Schiff Bases

AUTHORS: Sefa Durmus,Aslihan Dalmaz,Mesut Özdiñer,Sezen Sivrikaya

PAGES: 25-30

ORIGINAL PDF URL: <https://dergipark.org.tr/tr/download/article-file/263928>

Preparation of Cerium Oxide Nanoparticles: An Efficient Catalyst to the Synthesis of Dimeric Disulphide Schiff Bases

Sefa Durmus¹, Aslihan Dalmaz^{1*}, Mesut Ozdincer², Sezen Sivrikaya³

¹Department of Chemistry, Faculty of Arts and Sciences, Duzce University, Duzce 81620, Turkey
aslihandalmaz91@gmail.com

²Department of Composite & Materials, Faculty of Technology, Duzce University, Duzce 81620, Turkey

³Department of Polymer Engineering, Faculty of Technology, Duzce 81620, Turkey

* Corresponding author

Received: 5th November (Kasım) 2016

Accepted: 21st December (Aralık) 2016

DOI: <http://dx.doi.org/10.18466/cbujos.282116>

Abstract

Dimeric disulphide Schiff bases were synthesized via reactions of 2,2'-diaminodiphenyl disulphide with various aromatic aldehydes under reflux and prepared nano-sized cerium oxide as catalyst. It was observed that, when nanocatalyst was used, the catalyst could be reduced the reaction time and increased yields compared with the none-catalyst conditions. Moreover, the CeO₂ nanocatalyst was easy preparation, non-hazardous, eco-friendliness and low cost. The morphological features of CeO₂ nanocatalyst were characterized by X-ray diffraction (XRD), scanning electron microscopy (SEM), energy dispersive X-ray (EDX). The structures of ligands were illuminated some techniques such as fourier transform infrared (FT-IR), nuclear magnetic resonance (NMR) spectroscopy and thermogravimetric analysis (TGA) / differential thermal analysis (DTA).

Keywords — Catalyst, Dimeric, Disulphide, Lanthanide Oxide, Nanoparticles, Schiff Base.

1 Introduction

Lanthanide oxide nanoparticles have been received considerable importance in synthetic chemistry owing to their specific features including high surface areas, high dispersion property, physical and chemical stability, non-toxicity and cost-effectiveness [1-4]. In this context, lanthanide oxide nanocatalyst have received a great deal of attention as they are cheap and easily obtainable and high catalytic activity [4] reused for several cycles, easily separable from the reaction mixtures. Among the various lanthanide oxide nanoparticles, cerium oxide-based catalysts are widely used as effective oxidation systems due to their unique properties such as redox, oxygen release and storage abilities [5-8].

Compounds that contain disulphide bonds in their structure, such as the dimeric disulphide Schiff bases, which are biologically and pharmacologically active molecules [9-12]. There has been a growing interest in

recent years toward the crystal structures and synthesis of these molecules owing to their various biological, pharmacological such as a antibacterial [13, 14], antifungal, antimicrobial [15], antitumor, anti-oxidants [14, 16], electrochemical [17-19], optical [20] properties.

In this study, we focused on efficient method and catalytic activity of cerium oxide nanoparticles for the synthesis of dimeric disulphide Schiff bases. The prepared nanocatalyst was identified by XRD, SEM, EDX, FT-IR and Raman spectroscopy. Also the synthesized ligands were characterized by FT-IR, ¹H and ¹³C NMR spectroscopy and TGA / DTA.

2 Experimental

2.1 Materials and Methods

Ce(NO₃)₃ 6.H₂O (Acros), 2-aminothiophenol (Merck), 5-bromo-2-hydroxy benzaldehyde (Merck), NaOH (Merck), EtOH (Merck), dimethyl sulfoxide (DMSO)

(Merck), chloroform (Merck), 2-hydroxy-1-naphthaldehyde (Sigma Aldrich) were used without further purification.

The synthesized CeO₂ nanoparticles were subjected to X-ray diffraction studies [using a Panalytical diffractometer and a Cu K α radiation source] to determine the crystal phase composition. The formation and elemental compositions of CeO₂ nanoparticles were confirmed by scanning electron microscopy/an energy dispersed X-ray analysis which was carried out using FEI Quanta FEG 250. The infrared spectra of the samples were determined on Perkin Elmer Spectrum ATR in the range 4000 to 400 cm⁻¹. TGA/DTA curves were obtained using a Shimadzu DTG-60H instruments. The heating rate was 10 °C/min. ¹H NMR and ¹³C NMR were recorded on Bruker 400 MHz, 100 MHz spectrometers.

2.2 Preparation of CeO₂ Nanocatalyst

0.002 mmol of Ce(NO₃)₃·6H₂O was dissolved in 15 ml of distilled water and then 0.3 M NaOH solution were added slowly drop by drop into Ce(NO₃)₃·6H₂O solution with magnetic stirrer until the mixture immediately turned into a pale yellowish. As seen in Figure 1, the obtained solution was centrifuged for 20 minutes, washed several times with distilled water and eventually dried at 300 °C for 3 hours.

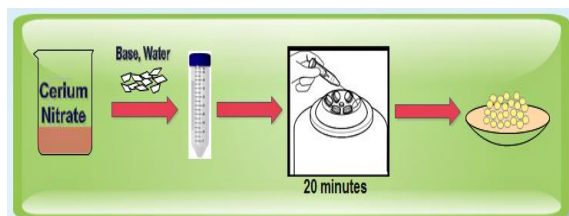


Figure 1. Schematic representation of the formation of CeO₂ nanoparticles by hydroxide mediated approach.

2.3 Synthesis of Schiff Bases

2.3.1 Synthesis of Schiff Bases without Catalyst

Ligands L₁-L₂ were synthesized by mixing a solution of 2,2'-diaminodiphenyl disulphide (1 mmol) and aromatic aldehydes (2 mmol) in absolute ethanol [21]. The reaction mixture was refluxed at room tempera-

ture and the progress of the reaction was monitored by thin layer chromatography (TLC). After completion of the reaction, the reaction mixture was filtered and then recrystallized in DMSO to afford pure product.

2.3.2 Synthesis of Schiff Bases with Nanocatalyst

2-aminophenyl disulphide (1 mmol) was dissolved in ethanol, followed by addition of aromatic aldehydes (2 mmol). The CeO₂ nanocatalyst was added to the reaction mixture and the reaction mixture was stirred until completion of the reaction. After the reaction was completed, the nanocatalyst was separated, washed several times with ethanol and then dried in oven. Thio Schiff base was washed with chloroform and then dried. The obtained ligands were purified by recrystallization from DMSO, as seen in Figure 2.

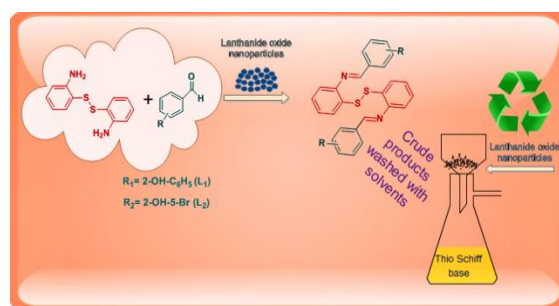


Figure 2. The synthesis of Schiff bases catalyzed by CeO₂ nanoparticles.

3 Results and Discussion

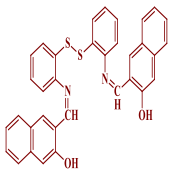
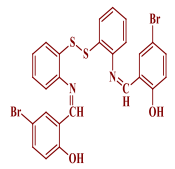
The images of obtained ligands were indicated in Figure 3. While the color of L₁ ligand has an orange, L₂ has a bright yellow. Furthermore, the melting points of the ligands for L₁ and L₂ were 210 °C and 182 °C, respectively.



Figure 3. The images of obtained L₁ and L₂ ligands.

Table 1. Comparison of reaction parameters (reaction time, yield) and NMR data of L₁ and L₂.

Product	Reaction Time		Yield		¹ H and ¹³ C NMR data (δ , ppm)
	Method A*	Method B**	Method A*	Method B**	
	(minute)		(%)		

L1		240	15	75	95
L2		360	15	87	98

*catalyst-free condition, **CeO₂ as a nanocatalyst.

¹H NMR (400 MHz, CDCl₃) δ 14.96 (s, 1H), 9.44 (s, 1H), 8.19 (d, *J* = 8.5 Hz, 1H), 7.89 (d, *J* = 9.1 Hz, 1H), 7.81 (d, *J* = 7.9 Hz, 1H), 7.73 (d, *J* = 7.8 Hz, 1H), 7.57 (t, *J* = 8.3 Hz, 1H), 7.43 – 7.37 (m, 1H), 7.26 – 7.20 (m, 4H) ppm.

¹³C NMR (100 MHz, DMSO): δ 164.8, 158.7, 145.1, 136.1, 132.6, 129.4, 128.9, 128.6, 128.0, 127.6, 127.4, 127.2, 123.7, 120.8, 119.9, 119.0, 109.4 ppm.

¹H NMR (400 MHz, CDCl₃) δ 12.85 (s, 1H), 8.55 (s, 1H), 7.66 (dd, *J* = 7.7, 1.4 Hz, 1H), 7.53 (d, *J* = 2.3 Hz, 1H), 7.48 (dd, *J* = 8.8, 2.3 Hz, 1H), 7.30 – 7.19 (m, 2H), 7.16 – 7.10 (m, 1H), 6.96 (d, *J* = 8.8 Hz, 1H) ppm.

¹³C NMR (100 MHz, CDCl₃) δ 161.4, 160.1, 146.2, 136.2, 134.5, 131.7, 128.0, 128.0, 128.0, 120.5, 119.5, 117.7, 110.6 ppm.

3.1 Phase Identification by XRD

The XRD pattern was used to determine the crystal phases of the synthesized CeO₂ nanoparticles. The X-ray pattern of the synthesized sample was depicted in Figure 4. The presence of CeO₂ could be confirmed by the characteristic reflection peaks at 2θ of 28.53°, 33.08°, 47.43°, 56.41°, 58.89°, 69.51°, 76.75°, 78.69°, 88.66° which were indexed as (111), (200), (220), (311), (222), (400), (331), (420) and (422) respectively. All the diffraction peak in the CeO₂ pattern corresponds well to the single phase body centered cubic, and it is in a good agreement with the pattern JCPDS file no 98-026-2755. The CeO₂ the lattice constant of CeO₂ is a=b=c=5.403 Å. The cell volume and space group of CeO₂ was 157.69 (Å)³ and Ia-3d, respectively. The data were obtained with JCPDS file no 98-026-2755. No characteristic peak of impurities was detected in the XRD patterns.

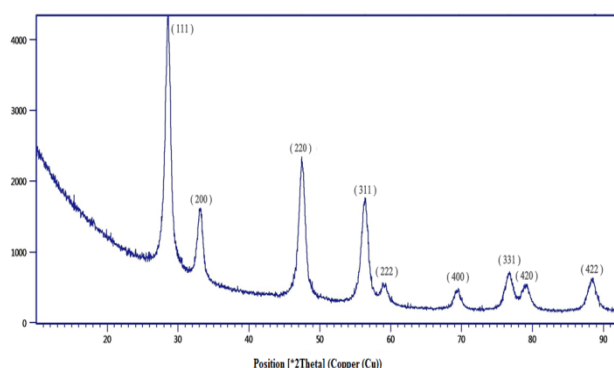


Figure 4. XRD pattern of prepared CeO₂ nanoparticles.

The SEM images proved that particles of sample were approximately spherical in shape and their size distribution was uniform with the particle size in nanoscale. In addition, the particle sizes of CeO₂ were observed to 18-37 nm based on SEM images, as seen in Figure 5.

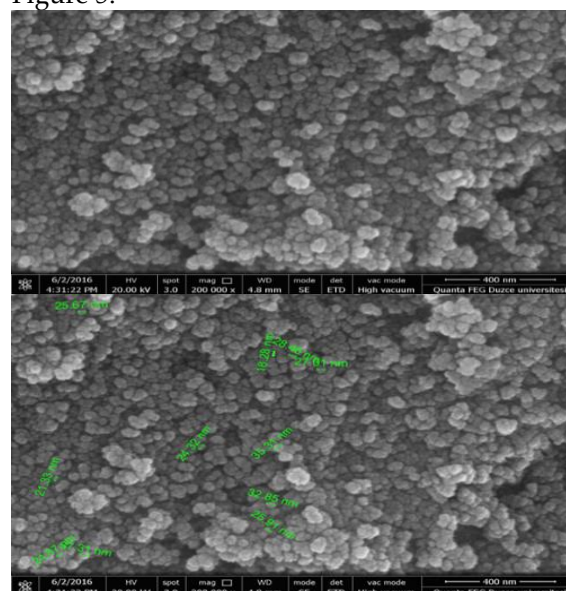


Figure 5. SEM images of CeO₂ nanoparticles.

The structural composition of prepared CeO₂ nanoparticles were examined by EDX as indicated in Figure 6. EDX proved that there were no other elements out of cerium and oxygen atoms. According to the EDX spectrum, prepared CeO₂ nanoparticles were pure and had not free of any surfactant or impurity.

3.2 Microstructural Characterization

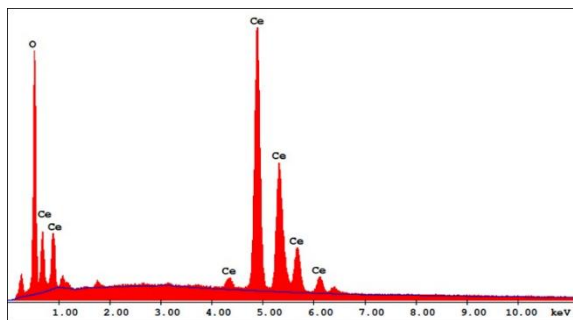


Figure 6. EDX image of CeO₂ nanoparticles.

3.3 Spectroscopic Characterization

As seen in Figure 7, the infrared spectra of the ligands (L₁-L₂) exhibited characteristic strong intensity bands in the region of 1620-1609 cm⁻¹ which were assigned to azomethine group $\nu(\text{C}=\text{N})$ stretching frequency. Moreover the bands attributed to $\nu(\text{Ar}-\text{C}=\text{C})$ at 1460, 1462 cm⁻¹; $\nu(\text{Ar}-\text{C}-\text{O})$ at 1243, 1276 cm⁻¹; and $\nu(\text{C}-\text{S})$ at 743, 735 cm⁻¹ were appeared, respectively. The characteristic frequency of disulphide bonds $\nu(\text{S}-\text{S})$ was appeared at 579 and 557 cm⁻¹, respectively. When the Figure 7 (b) was examined, $\nu(\text{C}-\text{Br})$ peak was observed at 624 cm⁻¹.

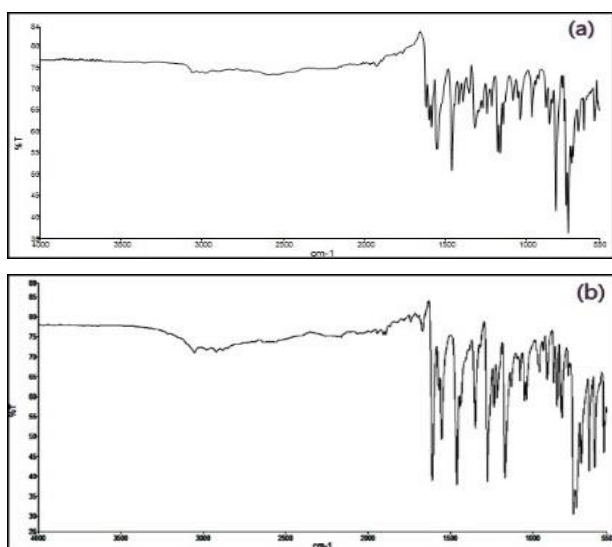


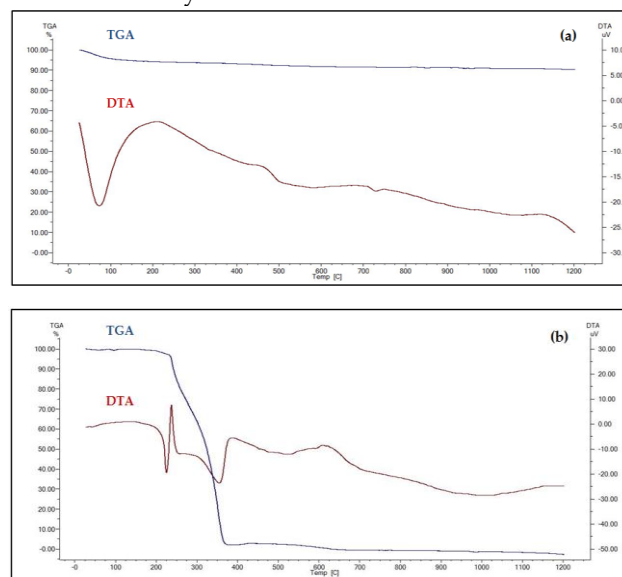
Figure 7. The FT-IR spectra of (a) L₁ and (b) L₂ ligands.

According to the ¹H NMR spectra of ligands (L₁-L₂), the hydroxyl protons appeared as a singlet at 14.96 and 12.86 ppm corresponding to the phenolic -OH, respectively. The azomethine proton (-HC=N) of the ligands resonated as a sharp singlet signal at 9.43 (for L₁) and 8.53 (for L₂) ppm. Furthermore, the multiple signals between 8.19 and 7.10 ppm with different multiplicity and coupling constants suggested the attribution of the protons of aromatic benzene rings.

All of the protons were found to be in their expected region and numbers and were compatible with literature values [22].

According to the signals for the ¹³C NMR of the Schiff bases, azomethine carbon resonances were observed in the range 160.1-158.7 ppm. Furthermore, the ¹³C NMR data confirmed the structures as indicated in Table 1.

The stability of the prepared CeO₂ nanoparticles was determined using TGA with flow rate N₂ of 50 mL per minute. As shown in Figure 8 (a), the thermogram of CeO₂ nanoparticles showed that a mass loss between 120 °C and 250 °C was associated with the hydration due to loss of water. Above 200 °C, no weight loss was observed and then it was thermally stable. The ligand (L₁) was stable about 210 °C and its decomposition started at this temperature. According to the DTA curve, the endothermic peak was observed due to the melting process of the ligands (for L₁) in the range of 216-220 °C and other (for L₂) in the range of 180-200 °C. The thermograms of ligands indicated that the decomposition of the ligands had one step and their weight loss was about 80 percent. The melting point of the synthesized ligands was compatible with TGA analysis.



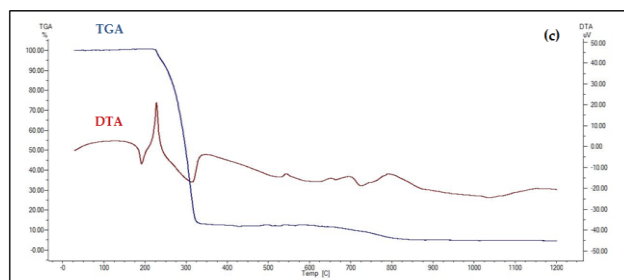


Figure 8. TGA / DTA diagrams of as-prepared (a) CeO₂ nanoparticles, (b) L₁ and (c) L₂ ligands.

4 Conclusions

In summary, dimeric disulphide Schiff bases were successfully prepared by both catalyst free condition and CeO₂ nanoparticles as a catalyst. The prepared CeO₂ nanocatalyst was an efficient and recyclable catalyst and its catalytic effect towards to synthesis of Schiff bases were investigated. The structure features of CeO₂ nanocatalyst were characterized by microscopic and spectroscopic methods.

The salient features of the present method are shorter reaction time, mild reaction conditions, reusability of the catalyst, easily available reagent and applicability to a wide range of ligands. In comparison with the catalyst-free condition, the reaction rate and yield were increased when the reaction was carried out in the presence of the catalyst.

Acknowledgements

This research was supported by Duzce University Scientific Research Fund (BAP) (Project No: 2014-05-03-259 and 2015-05-03-354).

5 References

- [1] Amini, M.; Hassandoost, R.; Bagherzadeh, M.; Gautam, S.; Chae, K.H. Copper Nanoparticles Supported on CeO₂ as an Efficient Catalyst for Click Reactions of Azides with Alkynes. *Catal. Commun.* 2016; 85, 13-16.
- [2] Shelkar, R.S.; Balsane, K.E.; Nagarkar, J.M. Magnetically Separable Nano CeO₂: A Highly Efficient Catalyst for Ligand Free Direct C–H Arylation of Heterocycles. *Tetrahedron Lett.* 2015; 56, 693-699.
- [3] Taguchi, M.; Ishikawa, Y.; Kataoka, S.; Naka, T.; Funazukuri, T. CeO₂ Nanocatalysts for the Chemical Recycling of Polycarbonate. *Catal. Commun.* 2016; 84, 93-97.
- [4] Wang, J.; Lou, Y.; Xu, C.; Song, S.; Liu, W. Magnetic Lanthanide Oxide Catalysts: An Application and Comparison in the Heterogeneous Catalytic Ozonation of Diethyl Phthalate in Aqueous Solution. *Sep. Purif. Technol.* 2016; 159, 57-67.
- [5] Abdollahzadeh-Ghom, S.; Zamani, C.; Andreu, T.;

Epifani, M.; Morante, J.R. Improvement of Oxygen Storage Capacity Using Mesoporous Ceria–Zirconia Solid Solutions. *Appl. Catal., B* 2011; 108-109, 32-38.

[6] Qian, J.; Chen, Z.; Liu, C.; Lu, X.; Wang, F. Improved Visible-Light-Driven Photocatalytic Activity of CeO₂ Microspheres Obtained by Using Lotus Flower Pollen as Biotemplate. *Mater. Scien. Semicond. Process.* 2014; 25, 27-33.

[7] Wen, H.; Liu, Z.; Yang, Q.; Li, Y.; Yu, J. Synthesis and Electrochemical Properties of CeO₂ Nanoparticle Modified TiO₂ Nanotube Arrays. *Electrochim. Acta.* 2011; 56, 2914-2918.

[8] Izu, N.; Shin, W.; Murayama, N.; Kanzaki, S. Resistive Oxygen Gas Sensors Based on CeO₂ Fine Powder Prepared Using Mist Pyrolysis. *Sens. Actuators, B.* 2002; 87, 95-98.

[9] Amirasr, M.; Bagheri, M.; Farrokhpour, H.; Schenk, K.J.; Mereiter, K.; Ford, P.C. New Zn(II) Complexes with N₂S₂ Schiff Base Ligands. Experimental and Theoretical Studies of The Role of Zn(II) in Disulfide Thiolate-Exchange. *Polyhedron* 2014; 71, 1-7.

[10] Shafaatian, B.; Mousavi, S.S.; Afshari, S. Synthesis, Characterization, Spectroscopic and Theoretical Studies of New Zinc(II), Copper(II) and Nickel(II) Complexes Based on Imine Ligand Containing 2-Aminothiophenol Moiety. *J. Mol. Struct.* 2016; 1123, 191-198.

[11] Amirasr, M.; Rasouli, M.; Mereiter, K. Copper(I) Complexes of New N₂S₂ Donor Schiff-Base Ligands Derived from 1,2-bis-(2-amino-phenylsulfanyl) ethane. *Inorg. Chim. Acta* 2013; 404, 230-235.

[12] Özdingör, M.; Atahan, A.; Durmuş, S. Synthesis and Structural Characterization of N₂S₂O₂ Type Dimeric Schiff Base, *J. New Results in Sci.* 2014; 4, 42-46.

[13] Bhowon, M.G.; Jhaumeer-Laulloo, S.; Soukhee, N.; Allibacus, A.; Shiboo, V. Synthesis, Catalytic and Antibacterial Activity of 2-Aminophenyldisulphide, *J. Coord. Chem.* 2007; 60, 1335-1343.

[14] Moosun, S.B.; Bhowon, M.G.; Hosten, E.C.; Jhaumeer-Laulloo, S. Crystal Structures, Antibacterial, Antioxidant and Nucleic Acid Interactions of Mononuclear, and Tetranuclear Palladium(II) Complexes Containing Schiff Base Ligands, *J. Coord. Chem.* 2016; 69, 2736-2753.

[15] Narain, Y.; Jhaumeer-Laulloos, S.; Bhowon, M.G.; Structure-activity Relationship of Schiff Base Derivatives of Bis(aminophenyl)disulfide and p-Vanillin as Antimicrobial agents. *Int. J. Biol. Chem. Sci.* 2010; 4, 69-74.

[16] Moosun, S.B.; Jhaumeer-Laulloo, S.; Hosten, E.C.; Gerber, T.I.A.; Bhowon, M.G. Antioxidant and DNA Binding Studies of Cu(II) Complexes of N,N'-(1,1'-dithio-bis(phenylene))-bis(salicylideneimine): Synthesis and Characterization, *Transition Met. Chem.* 2015; 40, 445-458.

[17] Temel, H.; Pasa, S.; Ocak, Y.S.; Yilmaz, I.; Demir, S.; Ozdemir, I. Synthesis, Characterization, Electrochemical Behaviors and Applications in the Suzuki–Miyaura Cross-coupling Reactions of N₂S₂O₂ Thio Schiff Base Ligand and Its Cu(II), Co(III), Ni(II), Pd(II) Complexes and Their Usage in the Fabrication of Organic–inorganic Hybrid Devices. *Synth.*

Met. 2012; 161, 2765-2775.

[18] Behpour, M.; Ghoreishi, S.M.; Honarmand, E.; Salavati-Niasari, M. A novel N,N'-[1,1'-Dithiobis(phenyl)]bis(salicylaldehyde) Self assembled Gold Electrode for Determination of Dopamine in the Presence of High Concentration of Ascorbic Acid. J. Electroanal. Chem. 2011; 653, 75-80.

[19] Gili, P.; Martin-Reyes, M.G.; Zarza, P.M.; Machado, I.L.F.; Guedes da Silva, M.F.C.; Lemos M.A.N.D.A.; Pombeiro, A.J.L. Synthesis, Spectroscopic, Magnetic and Electrochemical Properties of Cu(II) and Fe(III) Complexes with the New Ligand N,N'-[1,1'-dithiobis(phenyl)]bis(5'-methoxysalicylaldehyde). Inorg. Chim. Acta 1996; 244, 25-36.

[20] Khanmohammadi, H.; Rezaeian, K.; Amini, M.M.; Ng, S.W. Azo-azomethine Dyes with N, O, S Donor Set of Atoms and Their Ni(II) Complexes: Synthesis, Characterization and Spectral Properties. Dyes and Pigments 2013; 98, 557-564.

[21] Synthesis of 2,2'-diaminodiphenyl disulphide: 2,2'-diaminodiphenyl disulphide was synthesized by oxidation of 2-aminothiophenol.

[22] Donzelli, A.; Metushi, I.; Potvin, P.G. Titanium(IV) Complexes of Disulfide-linked Schiff Bases. Inorg. Chem. 2012; 51, 5138-45.